†Work supported by ARPA and the NSF through the Materials Science Program, Brown University.

*Present address: Division of Engineering, Brown University, Providence, R. I. 02912.

‡Present address: Notre Dame Radiation Laboratory, Notre Dame, Ind.

§Present address: National Bureau of Standards, Washington, D.C. 20234.

[1]W. Hanle, Z. Phys. **30,** 93 (1924).

[2]E. B. Saloman, Phys. Rev. **144,** 23 (1966).

[3]E. B. Saloman, Phys. Rev. **152,** 79 (1966).

[4]C. H. Corliss and W. R. Bozman, Natl. Bur. Std. Monograph No. 53 (U. S. GPO, Washington, D. C., 1962).

[5]C. H. Corliss, Natl. Bur. Std. Monograph No. 32 Suppl. (U. S. GPO, Washington, D. C., 1967).

[6]P. F. Gruzdev, Opt. Spektrosk. **25,** 3 (1968) [Opt. Spectrosc. **25,** 1 (1968)].

[7]N. P. Penkin, and I. Yu. Yu. Slavenas, Opt. Spektrosk. **25,** 3 (1968) [Opt. Spectrosc. **15,** 83 (1963)].

[8]P. A. Franken, Phys. Rev. **121,** 508 (1961).

[9]W. Happer and E. B. Saloman, Phys. Rev. **160,** 23 (1967).

[10]A. Omont, J. Phys. (Paris) **26,** 26 (1965).

[11]M. I. D'Yakonov and V. I. Perel', Zh. Eksp. Teor. Fiz. **48,** 345 (1965) [Sov. Phys.-JETP **21,** 227 (1965)].

[12]E. B. Saloman, A. Baghdadi, and J. B. Halpern, Rev. Sci. Instrum. **41,** 1148 (1970).

[13]A. Mitchell and M. Zemansky, *Resonance Radiation and Excited Atoms* (Cambridge U. P., Cambridge, England, 1961).

[14]J. P. Barrat, J. Phys. Radium **20,** 541 (1959); J. Phys. Radium **20,** 633 (1959).

[15]E. B. Saloman, thesis (Columbia University, 1965) (unpublished).

[16]W. J. Sandle and O. M. Williams, J. Phys. B **4,** 531 (1971).

[17]E. B. Saloman and W. Happer, Phys. Rev. **144,** 7 (1966).

PHYSICAL REVIEW A VOLUME 7, NUMBER 2 FEBRUARY 1973

# Determination of the Rydberg Constant from the He II $n = 3$-4 (469-nm) Line Complex

E. G. Kessler, Jr.

*Institute for Basic Standards, National Bureau of Standards, Washington, D. C. 20234*

(Received 28 August 1972)

The Rydberg constant has been determined from absolute wavelength measurements on two fine-structure components of the He II $n = 3$-4 transition. The He II transition was excited in a liquid-nitrogen-cooled hollow cathode. A pressure-scanned Fabry–Perot spectrometer was used to compare the He II wavelengths with a $^{198}$Hg standard source. The measured value of the Rydberg is $R_\infty = 109\,737.3208 \pm 0.0085$ cm$^{-1}$, where the uncertainty is one standard deviation.

## I. INTRODUCTION

The presently accepted value of the Rydberg[1] is based on wavelength measurements on H, D, and He II by Houston,[2] Chu,[3] Drinkwater, Richardson, and Williams,[4] and Csillag.[5] Because of advances in spectroscopic techniques and in our understanding of one-electron atoms, the more recent measurements of Csillag on six deuterium lines $D_\beta - D_\eta$ are less susceptible to systematic errors and show a smaller statistical error than the earlier data. Additional wavelength measurements on hydrogen and hydrogenlike lines have recently been undertaken by several experimenters to provide additional spectroscopic data for a Rydberg determination.[6–8] Absolute wavelength measurements on the two best resolved fine-structure components in the He II $n = 3$-4 ($\lambda = 469$-nm) line complex in $^4$He are reported here.

## II. He II $n = 3$-4 LINE COMPLEX

The fine structure of the He II $n = 3$-4 transition is illustrated in Fig. 1. The 13 fine-structure components have been numbered in order from high to low wave number to facilitate discussion. Recent high-resolution studies of this transition which were concentrated on relative position and intensity measurements and discharge processes have provided information on intensity anomalies, differential Doppler shifts, stark shifts, and anomalously large component widths.[9–11] This information has been very helpful in the selection of discharge parameters (current, pressure, cathode diameter, and position of cathode and anode relative to the spectrometer) which produce a relatively unperturbed He II spectrum and thus reduce systematic errors.

The advantages of measuring He II transitions as compared to hydrogen lines are a reduction in the Doppler width and more isolated individual components. However, these advantages are offset by the weak He II line intensities relative to hydrogen line intensities and the presence of an ion which is more susceptible to systematic errors. In Refs. 10 and 11, component positions were observed to depend on the orientation of the anode and cathode relative to the spectrometer. A differential Doppler shift is superimposed on the random Doppler motion because the positively charged He ion drifts toward the cathode. To correct for any differential Doppler shift, double-anode hollow cathodes have been employed which allow measurements to be recorded with the ions drifting toward and away from the spectrometer.[11] In addition, cathode parameters

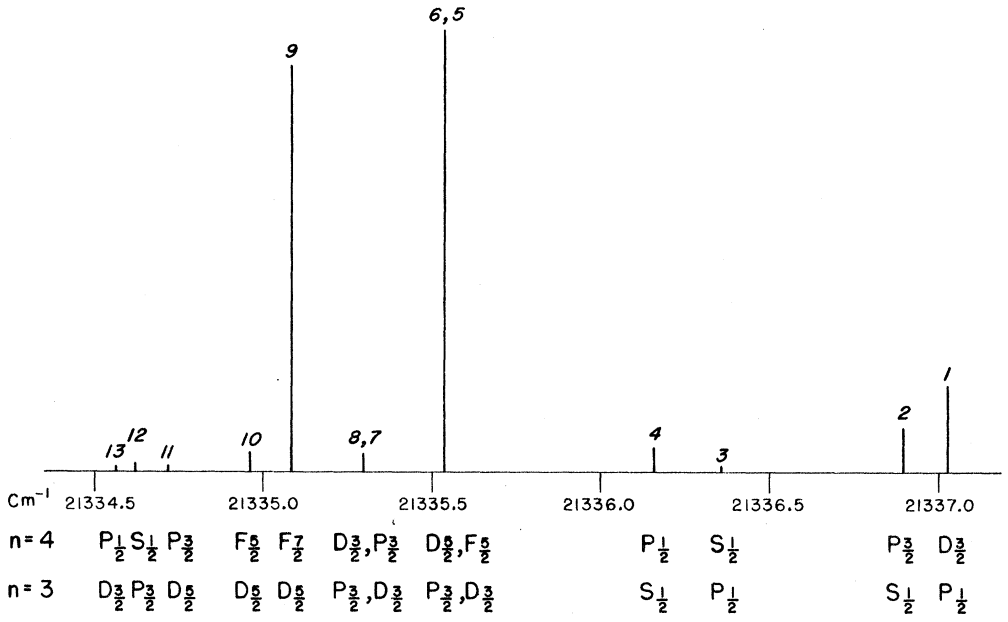


FIG. 1. Fine structure of the He II $n=3$-4 (469-mm) transition. The lengths of the vertical lines indicate theoretical relative intensities.

(diameters >15 mm and pressures >0.3 Torr) were chosen to suppress the differential Doppler shift. No differential Doppler shift was detected in any of the data used for Rydberg determination.

Because of the spacing and intensity distribution of the components, the wavelengths of components 5+6 and 9 can be more accurately measured than those of the other ten components. These are the only two components on which absolute wavelength measurements were made.

The discharge tube was cooled in liquid nitrogen in order to reduce the Doppler width and improve the resolution. Liquid-nitrogen rather than liquid-helium cooling was used because liquid-helium cooling significantly increases the difficulty of the experiment while reducing the linewidth to only 0.8 times the linewidth obtained for liquid-nitrogen cooling.

## III. INSTRUMENTATION

A pressure-scanned Fabry–Perot spectrometer with photoelectric detection and digital readout was used to compare the unknown wavelengths to a standard. The instrument is shown schematically in Fig. 2 and is discussed in detail in the literature.[8,12,13]

Even though only the wavelengths of components 5+6 and 9 were measured, knowledge of the entire He II $n=3$-4 spectrum produced by the discharge is essential to aid in the decomposition and to ensure that there were no anomalous discharge phenomena. For recordings of all 13 components of the He II $n=3$-4 transition, the He II radiation passed through the two Fabry–Perot etalons $E_1$ and $E_2$ which were both pressure scanned. Dry nitrogen was used as the scanning gas. Figure 3 shows a typical double-etalon scan.

The resolving etalon $E_1$ had a plate separation of

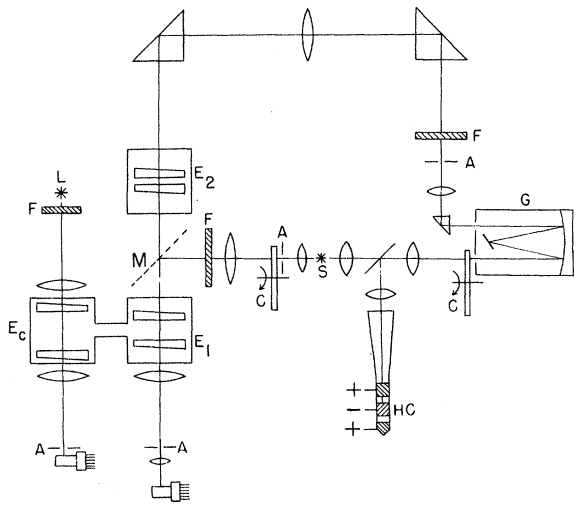


FIG. 2. Sources and spectrometer. $E_1$, $E_2$, and $E_c$ are the resolving etalon, suppression etalon, and calibration etalon, respectively. The other parts are F, filters; C, choppers; A, circular apertures; G, grating premonochromator; M, partially reflecting mirror; HC, hollow cathode; S, standard source; and L, calibration lamp.

6.0 mm, 4.5 mm, or 3.0 mm, while the suppression etalon $E_2$ always had a plate separation of 1.3 mm. Two etalons are necessary to provide an instrumental width of 0.030 to 0.050 $cm^{-1}$ while suppressing overlapping orders.

Absolute wavelength measurements of the 5+6 and 9 components are determined by the method of exact fractions, which requires recording two or more Fabry–Perot orders.[14] Because double-etalon systems in which both etalons are scanned suppress repeated orders, a system in which only one etalon is scanned must be used. Etalon $E_1$ was pressure scanned, while etalon $E_2$ was held at a constant pressure and served as a tunable filter of approximately 0.135-$cm^{-1}$ halfwidth to isolate components 5+6 and 9 of the 469-nm structure. Tuning was accomplished by adjusting the pressure in etalon $E_2$ for maximum transmission of the component under study. Spectra obtained in this way are shown in Fig. 4. These recordings are free of overlap except for the slight presence of component 9 in the recording of component 5+6 and vice versa. Two or three orders were recorded in each scan and the time per scan was approximately 50 min.

The standard-wavelength source was a water-cooled $^{198}$Hg electrodeless discharge lamp $S$, which was constructed and operated in accordance with the Comité Consultatif pour la Définition de Mètre (CCDM) specifications.[15] The $^{198}$Hg 546-nm line was used as standard for all measurements, but a few scans of the 577- and 579-nm lines were recorded with each spacer so that integer order numbers could be unambiguously determined. Light from the standard lamp was passed through etalon $E_1$ simultaneously with the He II radiation. Simultaneous scanning eliminates systematic errors resulting from drift and misalignment of the etalon plates. The standard and the He II light beams were equipped with choppers at two different frequencies so that the two light signals could be detected by one photomultiplier used in conjunction with two lock-in detectors.

The standard lamp radiation could also be passed through the same optical train as the He II spectrum. Thus by observing coincidence of two $^{198}$Hg line fringes, one from each of the two arms of the spectrometer, instrumental shifts including electronic shifts between the two arms of the spectrometer could be monitored and corrected.

A third long-spaced (5 cm) etalon $E_c$ was scanned simultaneously with etalon $E_1$. Fringes produced by this etalon were detected by a second photomultiplier and provided a means of correcting for nonlinearity of the scan rate and a wave-number scale for double-etalon scans of the 469-nm line.

Fabry–Perot interferometers which are used to measure precision absolute wavelengths are usually coated with metallic coatings because the disper-

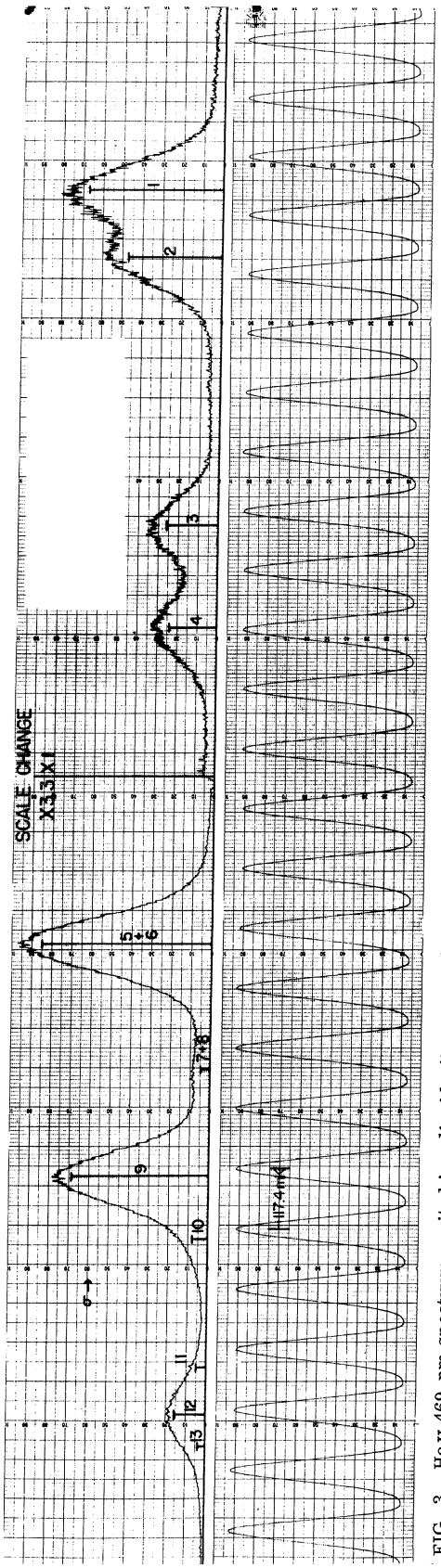


FIG. 3. He II 469-nm spectrum excited in a liquid-nitrogen-cooled aluminum hollow cathode. The current was 10-mA, and the pressure was 0.5 Torr. The peak-to-peak separation of the calibration sine curve is 0.1174 $cm^{-1}$.

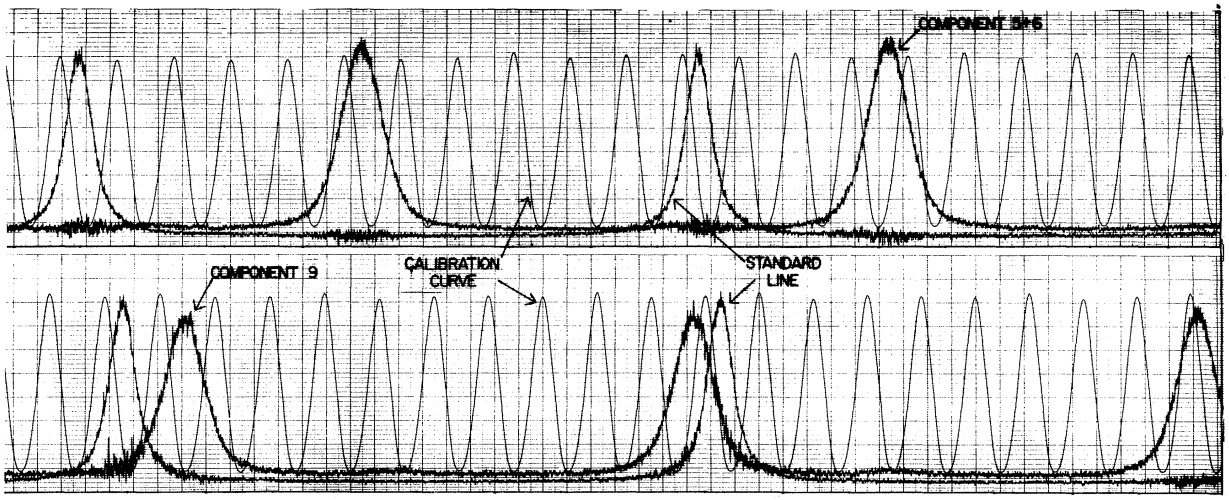


FIG. 4. Single etalon scans of the He II 469-nm line excited in a liquid-nitrogen-cooled hollow cathode. The pressure in etalon $E_2$ was adjusted to isolate component 5+6 and component 9 in the upper and lower scans, respectively. The discharge current was 10 mA and the pressure was 0.5 Torr. The standard wavelength was the 546-nm line excited in a water-cooled $^{198}$Hg electrodeless lamp. The sine curve provides interferometric calibration of the spectrum; the peak-to-peak separation is 0.1174 $cm^{-1}$ for the He II spectrum and 0.1001 $cm^{-1}$ for the standard line.

sion of phase change for these coatings is small. However, because of the low light levels available in this experiment, multilayer dielectric coatings which combine high reflectance, low absorption, and large dispersion of phase have been employed. By taking data at several different separations of the same etalon plates, any dispersion of the phase change which results from the multilayer dielectric coatings can be eliminated.[16] The coatings had a reflectance of 95–96% from 450 to 560 nm. The useful diameter of the plates was 4.5 cm.

## IV. DATA ANALYSIS

To determine fractional orders, the positions of the standard and the He II fringes were measured relative to a reference pressure of 0.03 Torr. Numerical profiles were obtained for the standard line source and the He II component by averaging the profiles of several recorded peaks of each source and consist of a set of $x$ and $y$ coordinates which represent the shape of the line passed by the instrument. These profiles exhibited a slight asymmetry with the red wing being slightly higher than the blue wing. The positions of the fringes were then determined by computer fitting each order with the numerical profile having an adjustable position, intensity, and width. The least-squares criterion was used to obtain the best fit. Figure 5 illustrates the quality of fit of a typical scan.

In the analysis of scans of component 5+6, the incompletely suppressed component 9 was included with an adjustable intensity, but with a fixed position relative to component 5+6 and with a width equal to that of component 5+6. To ensure that all other suppressed components were not detectable, a few recordings were analyzed with all components included. Intensities were allowed to vary, but positions were fixed relative to component 5+6, and widths were set equal to that of component 5+6. The intensities of all suppressed components were found to be negligible.

The procedure for the determination of the peak positions of component 9 was similar to that used for component 5+6. However, component 10, which lies 0.122 $cm^{-1}$ to the red of component 9 and is approximately $\frac{1}{20}$ as intense, was included with a fixed position relative to component 9, a width

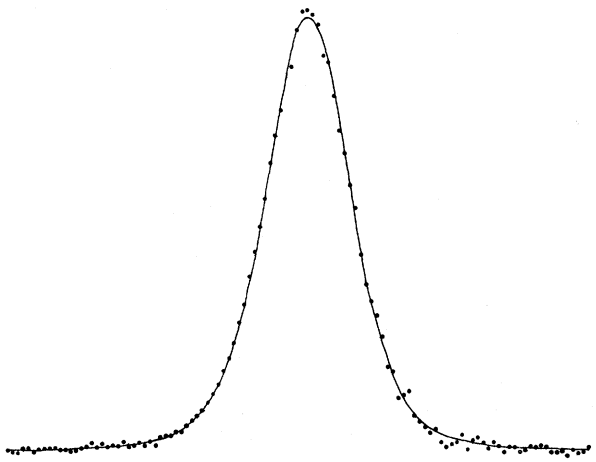

FIG. 5. Computed fit of one order of component 5+6 of the He II 469-nm line. The dots represent the data points and the solid line is the computed spectrogram.

TABLE I. Measured order numbers for component 5+6.

| Date | Spacer (mm) | Standard order numbers | He II order numbers |
|---|---|---|---|
| 1 | 6.0 | 22125.037 98 | 25784.717 30 |
| 1 | 6.0 | 22125.037 48 | 25784.716 52 |
| 2 | 6.0 | 22125.036 35 | 25784.717 70 |
| 2 | 6.0 | 22125.043 20 | 25784.724 48 |
| 2 | 6.0 | 22125.041 42 | 25784.722 59 |
| 2 | 6.0 | 22125.040 53 | 25784.721 74 |
| 4 | 6.0 | 22124.999 63 | 25784.674 57 |
| 4 | 6.0 | 22124.999 49 | 25784.675 17 |
| 5 | 6.0 | 22124.999 23 | 25784.675 12 |
| 5 | 6.0 | 22124.999 96 | 25784.675 54 |
| 6 | 4.5 | 16705.155 33 | 19468.360 39 |
| 6 | 4.5 | 16705.155 12 | 19468.359 07 |
| 6 | 4.5 | 16705.155 97 | 19468.359 00 |
| 6 | 4.5 | 16705.155 21 | 19468.358 08 |
| 7 | 4.5 | 16705.158 85 | 19468.361 97 |
| 7 | 4.5 | 16705.156 91 | 19468.361 68 |
| 7 | 4.5 | 16705.157 74 | 19468.361 58 |
| 7 | 4.5 | 16705.157 01 | 19468.362 34 |
| 8 | 3.0 | 11097.575 69 | 12933.258 72 |
| 8 | 3.0 | 11097.575 10 | 12933.257 69 |
| 8 | 3.0 | 11097.576 10 | 12933.258 31 |
| 9 | 3.0 | 11097.559 88 | 12933.243 79 |
| 9 | 3.0 | 11097.559 55 | 12933.243 45 |
| 10 | 3.0 | 11097.551 84 | 12933.232 56 |
| 10 | 3.0 | 11097.551 23 | 12933.232 66 |
| 10 | 3.0 | 11097.551 29 | 12933.232 59 |
| 10 | 3.0 | 11097.551 14 | 12933.232 76 |

equal to that of component 9, and a variable intensity. In double-etalon scans, component 10 causes a marked raising of the red wing of component 9, and the determination of its parameters using computer techniques presents no difficulty. However, the use of etalon $E_2$ as a filter centered on component 9 suppresses component 10 so that its intensity is only approximately 1% that of component 9.

The calculation of the fractional order from the two or three measured peak positions was performed using a least-squares procedure suggested by Meissner.[14]

## V. RESULTS

The absolute wave numbers of components 5+6 and 9 were based on 27 and 19 measured pairs of fractional orders, respectively. A pair of fractional orders consisted of one fractional order of the He II component and one fractional order of the standard line recorded simultaneously. The number of measured pairs for each spacer is as follows—component 5+6; 6.0-mm spacer-10, 4.5-mm spacer-8, 3.0-mm spacer-9: component 9; 6.0-mm spacer-7, 4.5-mm spacer-6, 3.0-mm spacer-6. The integral order numbers were determined in the usual way from the standard lines and were combined with the fractional orders. The measured order numbers are recorded in Tables I and II. The numbers in the date column refer to a particular calendar day on which measurements were made. The one standard deviation uncertainty in the measured order numbers was approximately ±0.000 15 and ±0.0003 for the standard and He II order numbers, respectively.

By taking differences between the order numbers measured at different spacer lengths, any errors due to the dispersion of phase change can be eliminated.[16] In this way 242 values (all possible different-spacer pairs) for the wave number of component 5+6 and 120 values for the wave number of component 9 can be found. The proper statistical method to combine these nonindependent wave-number measurements into one "best" value with a meaningful statistical error is not obvious. Thus, the following alternate statistically sound approach was adopted. The fundamental Fabry–Perot formula was applied to the case at hand to obtain

$$k_x = 2n_x\sigma_x(l+\tau_x),$$

$$k_s = 2n_s\sigma_s(l+\tau_s),$$

where $x$, $s$ refer to unknown and standard wave numbers, respectively, $k_{x,s}$ are the order numbers, $n_{x,s}$ are the indices of refraction, $\sigma_{x,s}$ are the wave numbers, $l$ is the mechanical spacer length, $\tau_{x,s}$ is the small-wave-number-dependent corrections to the spacer length resulting from dispersion of phase change. Let

$$l+\tau_s = \mathcal{E},$$

$$k_x = 2n_x\sigma_x(\mathcal{E}+\tau_x-\tau_s),$$

TABLE II. Measured order numbers for component 9.

| Date | Spacer (mm) | Standard order numbers | He II order numbers |
|---|---|---|---|
| 2 | 6.0 | 22125.042 15 | 25784.172 00 |
| 3 | 6.0 | 22125.040 38 | 25784.174 40 |
| 3 | 6.0 | 22125.040 43 | 25784.174 10 |
| 5 | 6.0 | 22124.997 71 | 25784.120 82 |
| 5 | 6.0 | 22124.996 66 | 25784.120 33 |
| 5 | 6.0 | 22124.998 06 | 25784.120 47 |
| 5 | 6.0 | 22124.996 83 | 25784.120 12 |
| 6 | 4.5 | 16705.154 81 | 19467.947 71 |
| 6 | 4.5 | 16705.155 10 | 19467.943 48 |
| 7 | 4.5 | 16705.156 58 | 19467.946 72 |
| 7 | 4.5 | 16705.156 12 | 19467.946 43 |
| 7 | 4.5 | 16705.156 77 | 19467.949 78 |
| 7 | 4.5 | 16705.156 36 | 19467.947 70 |
| 10 | 3.0 | 11097.550 39 | 12932.954 33 |
| 10 | 3.0 | 11997.549 58 | 12932.953 57 |
| 11 | 3.0 | 11097.551 32 | 12932.955 75 |
| 11 | 3.0 | 11097.550 42 | 12932.955 31 |
| 11 | 3.0 | 11097.550 17 | 12932.955 07 |
| 11 | 3.0 | 11097.549 88 | 12932.954 96 |

TABLE III. Measured fitting parameters.

| Component | Pairs of order numbers | $\alpha$[a] | $\beta$[a] |
|---|---|---|---|
| 5+6 | 27 | 1.165 404 9002 ± 660 | 0.090 66 ± 115 |
| 5+6 | 9 | 1.165 404 8775 ± 1047 | 0.091 16 ± 187 |
| 9 | 19 | 1.165 380 0277 ± 767 | 0.091 53 ± 134 |
| 9 | 7 | 1.165 380 0405 ± 1235 | 0.091 25 ± 223 |

[a]Uncertainties refer to last digits of main numbers.

TABLE IV. Comparison of experimental and theoretical wave numbers. Uncertainties quoted are statistical uncertainties only.

| Component | Experimental vacuum wave number ($cm^{-1}$) | Theoretical vacuum wave number ($cm^{-1}$) | expt-theory (ppm) |
|---|---|---|---|
| 5+6 | 21 335.5393 ± 0.0019 | 21 335.537 32 | +0.092 ± 0.089 |
| 9 | 21 335.0846 ± 0.0023 | 21 335.082 05 | +0.119 ± 0.106 |

and

$$k_s = 2n_s\sigma_s(\mathcal{E}) .$$

Then,

$$k_x = \alpha k_s + \beta ,$$

where

$$\alpha = n_x\sigma_x / n_s\sigma_s \qquad (1)$$

and

$$\beta = 2n_x\sigma_x(\tau_x - \tau_s) .$$

This linear equation was least-squares fitted to the 27 pairs and 19 pairs of order numbers to obtain values for $\alpha$ and $\beta$ (see Table III). From the values of $\alpha$, the unknown wave numbers can be determined. The values of $\beta$ provide a measure of the phase dispersion.

The 27 and 19 pairs of order numbers included measurements recorded on the same day and measurements recorded on different days. Careful inspection of the data showed that data recorded on the same day deviated approximately the same amount from the fitted line, while data recorded on different days deviated different amounts from the fitted line. In general, the data indicated that pairs of order numbers recorded on the same day were correlated. In order to take account of this correlation, the pairs of order numbers for a given day were averaged to obtain a pair of order numbers for that day. The 27 and 19 pairs of order numbers were reduced to 9 and 7 pairs, respectively, which were then least-squares fitted with linear equations to obtain values for $\alpha$ and $\beta$ (see Table III). The values of $\alpha$ from which the wave numbers are determined change by approximately 2 parts in $10^8$ as the pairs of order numbers were reduced from 27 and 19 to 9 and 7, respectively. The uncertainties given to $\alpha$ and $\beta$ are the statistical uncertainties as obtained from the least-squares fit. These uncertainties, as all uncertainties in this paper (statistical, systematic, and total uncertainties), are meant to represent one standard deviation. From the values of $\alpha$ for the 9 and 7 pairs of order numbers and Eq. (1), the wave numbers in Table IV, column 2 were calculated. From these wave numbers, the Rydberg was determined.

## VI. COMPUTATION OF THE RYDBERG

The procedure for computing the Rydberg from the measured wave numbers was similar to that used by Taylor, Parker, and Langenberg.[1] The measured wave numbers were compared with theoretical wave numbers calculated by Garcia and Mack.[17,18] The measured and theoretical wave numbers are given in columns 2 and 3, Table IV. Column 4 of Table IV gives the difference in parts per million between the experimental and theoretical wave numbers. The values for the Rydberg constant for He, $R_{\mathrm{He}}$, given in Table V, column 1, were obtained by altering the Garcia and Mack value for $R_{\mathrm{He}}$ by the experimental-theory difference.

Values for $R_\infty$ are determined from $R_{\mathrm{He}}$ by using the equation $R_\infty = R_{\mathrm{He}}(1 + m_e/M_\alpha)$. The quantity $(1 + m_e/M_\alpha) = 1.000\,137\,093\,4$[19] with an uncertainty of less than 1 in $10^9$. A weighted average of the two values for $R_\infty$ produced a final weighted average for $R_\infty$ which is $R_\infty = 109\,737.3208 \pm 0.0075\ cm^{-1}$ (statistical uncertainty only).

## VII. SYSTEMATIC ERRORS

The uncertainties assigned to the previously discussed wave number and Rydberg values include only statistical errors. Systematic errors associated with (1) uncertainties in the standard wavelength, (2) uncertainties in the indices of refraction at which fractional orders were measured, (3) un-

TABLE V. Computation of the Rydberg. Uncertainties quoted are statistical uncertainties only.

| Component | $R_{\mathrm{He}}$ ($cm^{-1}$) | $R_\infty$ ($cm^{-1}$) | Weighted average ($cm^{-1}$) |
|---|---|---|---|
| 5+6 | 109 722.2775 ± 0.0098 | 109 737.3197 ± 0.0098 | 109 737.3208 ± 0.0075 |
| 9 | 109 722.2804 ± 0.0116 | 109 737.3226 ± 0.0116 | |

certainties resulting from the blending of components, and (4) uncertainties resulting from the use of the tunable filter were investigated.

*a. Uncertainties in the standard wavelength.* The wavelength of the standard line, the $^{198}$Hg 546-nm line, was measured by comparison with the primary standard $^{86}$Kr 606-nm line after the He II-Hg comparison was completed. Any variation in the wavelength produced by the Hg lamp between the He II-Hg comparison and the Kr-Hg comparison is unlikely because of the low pressure and large reservoir of the Hg lamp. A pressure-scanned flat-plate Fabry–Perot interferometer with photoelectric detection was used to make this measurement. Spacers of 110, 66, and 44 mm were used to allow correction for dispersion of phase. The data analysis was identical to that employed in the He II-Hg comparison. The measured vacuum wavelength was 546.227 054 ± 0.000 007 nm, where the uncertainty includes statistical error and systematic error in the $^{86}$Kr lamp of 1 part in $10^8$. This measured wavelength is in excellent agreement with the value assigned to the secondary standard $^{198}$Hg 546-nm line by CCDM,[15] which is 546.227 05 nm to within 5 parts in $10^8$. The $^{198}$Hg 546-nm wave number used in all the calculations was 18307.405 17 ± 0.000 23 cm$^{-1}$. This uncertainty results in an uncertainty of ± 0.0014 cm$^{-1}$ in the Rydberg.

*b. Uncertainties in the indices of refraction.* The pressure, temperature, and dispersion formulas affect the values of the indices of refraction, $n_s$ and $n_x$. However, since the measured slope contains only the quotient $n_s/n_x$, uncertainties resulting from pressure and temperature are approximately 1 part in $10^9$. Also, the dispersion formula given by Peck and Khanna[20] provides relative values of the indices of refraction accurate to 1 part in $10^9$. Thus, no systematic error was included for pressure-, temperature-, and dispersion-formula uncertainties. The value of $n_s/n_x$ for a pressure of 0.03 Torr which was used in all calculations was 1.000 000 000.

*c. Uncertainties resulting from blending.* No attempt was made to resolve components 5 and 6 from the blend. These two components are theoretically separated by only 0.002 46 cm$^{-1}$. The measured peak position was assumed to be located at the center of gravity of components 5 and 6. From double-etalon scans of the entire He II $n = 3$-4 complex, the intensity of component 5 relative to component 6 can be inferred by using the measured intensities of components 9 and 1 and the theoretical multiplet intensity ratios. Theoretical intensity ratios within multiplets are known to be valid from the work of Roesler and Mack.[10] Thus, the theoretical wave number of the center of gravity of the blend, which will be compared to the measured wave number of the peak of the blend to determine the Rydberg, can be calculated from indirectly measured relative intensities of components 5 and 6 rather than assumed theoretical intensities. The coincidence of the peak of the blend and the center of gravity of components 5 and 6 is the only assumption employed. The uncertainty in the measured relative intensities of components 5 and 6 was approximately 5%. Thus, a systematic error of ± 0.0005 cm$^{-1}$ was included in the measured wave number of component 5 + 6. This uncertainty results in an uncertainty of ± 0.0026 cm$^{-1}$ in the Rydberg.

The discharge pressure for all data was 0.5 ± 0.05 Torr. In this pressure range, the relative intensities of all He II components were constant within the accuracy of measurement. The measured relative intensity of components 5 and 6 = 1.172. By using the theoretical wave numbers for components 5 and 6 given by Garcia and Mack,[17] the theoretical wave number for the 5 + 6 blend = 21 335.537 32 cm$^{-1}$.

Although component 10 distinctly raises the red wing of component 9, it shifts the peak position of the 9-10 blend only approximately 0.0001 cm$^{-1}$ from the peak of component 9. Thus, the peak of the 9 and 10 blend is for practical purposes the peak of component 9. The theoretical wave number[17] for component 9 = 21 335.082 05 cm$^{-1}$.

*d. Uncertainties resulting from the use of the tunable filter.* Etalon $E_2$, which serves as a tunable filter to isolate the component being measured, is centered on the component by maximizing its intensity. If the passband of the filter is not accurately centered on the component, the peak of the component may be shifted. The full width at half-maximum of etalon $E_2$ and the He II line are approximately 0.135 and 0.100 cm$^{-1}$, respectively. Because the filter function is 1.35 times as wide as the source function, the shifting of the source profile is reduced. Nevertheless, uncertainties of ± 0.0005 cm$^{-1}$ in the wave number might be introduced because intensity changes of less than 1% are difficult to detect. In an effort to reduce this systematic error or at least make it part of the statistical error, the tunable filter was retuned at the beginning of each recording. This uncertainty transforms into an uncertainty of ± 0.0026 cm$^{-1}$ in the Rydberg.

The statistical error of the final weighted average (Table V, column 4) and the above systematic errors were combined in the root-sum-square manner to obtain

$$R_\infty = 109\,737.3208 \pm 0.0085 \text{ cm}^{-1}.$$

This value of $R_\infty$ lies approximately one standard deviation from the presently accepted value[1] which is 109 737.312 ± 0.011 cm$^{-1}$. The presently accepted

value was obtained by (i) combining the measurements of Houston, Chu, and Drinkwater, Richardson, and Williams ($R_\infty = 109\,737.317\ cm^{-1}$); (ii) assigning the more recent measurement of Csillag ($R_\infty = 109\,737.307\ cm^{-1}$), a weight equal to that of the combined measurement in (i); and (iii) performing a weighted average of (i) and (ii). The value of $R_\infty$ obtained in this experiment differs significantly (approximately two standard deviations of the presently accepted value) from Csillag's measurement, the measurement carrying the most weight in the presently accepted value.

In 1970 Masui[6] made a Rydberg determination from two-beam interferograms of $H_\alpha$ and obtained a value of $R_\infty = 109\,737.327\ cm^{-1}$. He has reevaluated his data in an effort to correct possible intensity anomalies[21] and has obtained $R_\infty = 109\,737.320\ cm^{-1}$. The close agreement of the Rydberg reported here and that of Masui may be significant. However, more details concerning the intensity anomalies and the evaluation of the data must be made available by Masui.

A recent abstract by Kibble *et al.*[22] reports wavelength measurements on Balmer $\alpha$ in deuterium and tritium. From these measurements, a Rydberg of $109\,737.326 \pm 0.008\ cm^{-1}$ was deduced. This measurement appears to support the value of the Rydberg reported here.

## ACKNOWLEDGMENTS

I am grateful to the National Research Council-National Bureau of Standards for the postdoctoral research associateship during which most of this work was performed. I thank Dr. William Martin and Dr. Richard Deslattes for their continued interest in this work and many helpful discussions. William Bozman constructed the standard lamps. Dr. H. H. Ku provided assistance concerning the statistical analysis of the data. Robert Saunders of the Optical Radiation Section kindly supplied the data acquisition system and the lock-in amplifiers.

[1]B. N. Taylor, W. H. Parker, and D. N. Langenberg, Rev. Mod. Phys. **41,** 375 (1969).

[2]W. V. Houston, Phys. Rev. **30,** 608 (1927).

[3]D. Y. Chu, Phys. Rev. **55,** 175 (1939).

[4]J. W. Drinkwater, O. Richardson, and W. E. Williams, Proc. R. Soc. Lond. **174,** 164 (1940).

[5]L. Csillag, Acta Phys. Acad. Sci. Hung. **24,** 1 (1968).

[6]T. Masui, *Proceedings of the International Conference on Precision Measurement and Fundamental Constants,* Natl. Bur. Std. (U. S.) Spec. Publ. No. 343 (U. S. GPO, Washington, D. C., 1971), p. 83.

[7]B. Kibble, W. R. C. Rowley, and G. W. Series, *Proceedings of the Fourth International Conference on Atomic Masses and Fundamental Constants, Teddlington, England,* 1971 (Plenum, New York, 1971), p. 420.

[8]E. Kessler, Jr., in Ref. 7, p. 427.

[9]H. P. Larson and R. W. Stanley, J. Opt. Soc. Am. **57,** 1439 (1967).

[10]F. L. Roesler and J. E. Mack, Phys. Rev. **135,** A58 (1964).

[11]H. G. Berry and F. L. Roesler, Phys. Rev. A **1,** 1504 (1970).

[12]R. Chabbal, Rev. Opt. Theor. Instrum. **37,** 49 (1958).

[13]J. E. Mack, D. P. McNutt, F. L. Roesler, and R. Chabbal, Appl. Opt. **2,** 873 (1963).

[14]K. W. Meissner, J. Opt. Soc. Am. **31,** 405 (1941).

[15]Comité Intern. des Poids et Measures, Procès-Verbaux des Séances $2^e$ série **31,** 77 1963.

[16]R. W. Stanley and K. L. Andrew, J. Opt. Soc. Am. **54,** 625 (1964).

[17]J. D. Garcia and J. E. Mack, J. Opt. Soc. Am. **55,** 845 (1965).

[18]A more recent but yet unpublished calculation of wave numbers for one-electron spectra has been made by G. W. Erickson. This calculation differs from the Garcia and Mack calculation because slightly different values for the fundamental constants were used and additional quantum-electrodynamical terms were included. Because the values of the Rydberg that are determined from these two calculations are equal to within 5 parts in $10^9$, the published theoretical wave numbers of Garcia and Mack have been used throughout this paper.

[19]E. R. Cohen and B. N. Taylor, in Ref. 7, p. 543.

[20]E. R. Peck and B. N. Khanna, J. Opt. Soc. Am. **56,** 1059 (1966).

[21]T. Masui (private communication).

[22]B. P. Kibble, W. R. C. Rowley, G. W. Series, and R. E. Shawyer, Abstracts of Third International Conference on Atomic Physics (unpublished), p. 133.